Reconfigurable Transmitter Coil Structure for Highly Efficient and Misalignment-insensitive Wireless Power Transfer Systems in Megahertz Range*

*Lihao Wu and Bo Zhang**

(School of Electric Power, South China University of Technology, Guangzhou 510641, China)

Abstract: The structural optimization of coils is a key issue in wireless power transfer (WPT) applications owing to size limitations. In this study, a novel planar-spiral transmitter coil (TX-coil) with an outer-tight and inner-sparse configuration is proposed to achieve a high quality factor (Q-factor) and uniform magnetic field, which ensures high efficiency and improves the misalignment tolerance for several-megahertz WPT systems. Furthermore, a closed-form expression for the Q-factor is provided and analyzed for coil optimization. By using this method, a TX-coil with an outer diameter of 100 mm and a wire diameter of 1.5 mm is designed and tested at 1 MHz. Finite element method simulations and experimental results demonstrate that the Q-factor is increased by about 8% in comparison with evenly spaced planar spiral coils, which is achieved while ensuring a relatively uniform magnetic field.

Keywords: High quality factor, planar spiral coil, structure optimization, uniform magnetic field, wireless power transfer

1 Introduction

Wireless power transfer (WPT) technology has been widely used in various applications including electric vehicles, biomedical implants, and mobile phones [1-4], owing to its inherent advantages, such as a convenient, safe, and fully automated charging process. For commercial use of WPT technology, high efficiency and misalignment insensitivity are of a major significance. In addition, recently, many applications of WPT have been designed at a frequency higher than several megahertz, and have strict requirements on the size of the systems [4-5]. Therefore, the design of a proper coil under strict size constraints is essential for these applications.

For a certain transfer range, the quality factor (Q-factor) and uniformity of magnetic field for the transmitter coil (TX-coil) are two critical factors for the optimal efficiency and misalignment tolerance of WPT systems. A high Q-factor is important in maintaining high efficiency when the coupling coefficient is reduced due to misalignment or to an increased distance between the transmitter coil and receiver coil (RX-coil) [6]. Otherwise, the coupling coefficient will change slowly due to uniform magnetic field distribution, and then stable power transmission is certain regardless of RX-coil position[7].

Until now, many optimization methods have been reported to increase the Q-factor of the coils [5, 8-10]. In Ref. [8], multilayer helix coils made of litz wire were designed for a high Q-factor. Unfortunately, the influence of the proximity effect is significant for the litz wire above the MHz frequency range. Ref. [9] provides a design equation to calculate the Q-factor of spiral coils, and an optimized method of the printed spiral coils is presented in Ref. [10]. However, the proximity effect is not included in the design procedures of Refs. [9-10]. Therefore, their analysis and design methods are not suitable for the compact coils operating in the MHz frequency range. In Ref. [5], the volume filament model is used to calculate the ohmic resistance and inductance of the coils. By dividing a finite conductor into many filament wires, the skin and proximity effects can be reflected accurately in the calculation, but the magnetic field distributions are not considered in the optimization method. On another research front, much effort has been focused only on how to generate a uniform magnetic field distribution[11-13]. In Refs. [11-12], multiloop coils with unequal pitches were employed for free positioning in WPT systems, and the spatially structured resonant coil with a perpendicularly uniform magnetic field distribution was proposed in Ref. [13]. A high Q-factor and uniform magnetic field distribution have rarely been considered

* Corresponding Author, Email: epbzhang@scut.edu.cn
* Supported by the Key Program of National Natural Science Foundation of China (51437005).
Digital Object Identifier: 10.23919/CJEE.2019.000011

simultaneously in previous optimization or design methods.

In this study, a novel configuration of a multi-turn planar spiral TX-coil made of solid round wires is proposed to achieve a high Q-factor, as well as a relatively uniform magnetic field distribution to improve efficiency and misalignment tolerance of practical several-megahertz WPT applications. A closed-form expression for the Q-factor in terms of coil geometric parameters is provided and analyzed for coil optimization, and the skin effect and proximity effect are considered in the formula. The novelty of this work is to provide a simple design method with much lower computational cost than the finite element method (FEM).

2 Derivation of design equations

To simplify the calculation, we use a concentric annulus to model the spiral coil. All geometric parameters of the proposed coil are shown in Fig. 1. The pitches between inner turns (p_2) are larger than those between outer turns (p_1). Expressions for resistance, inductance, and Q-factor of the planar spiral coils are solved in terms of wire diameter w, the outer diameter d_{o1}, the number of outer turns and inner turns N_1 and N_2, and pitches p_1 and p_2 of the coil.

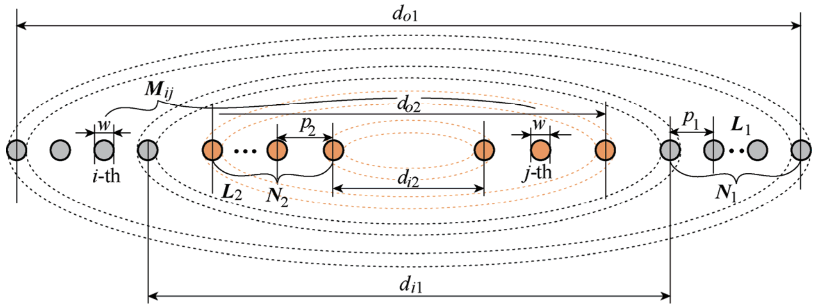

Fig. 1 Structure of the proposed planar spiral coils

2.1 Resistance

It is well known that the total AC resistance becomes greater than the DC resistance as the frequency increases, due to the skin and proximity effects, especially above the MHz frequencies. It is therefore necessary to consider the skin and proximity effects for the design of the coil under size constraints.

First, the resistance due to the skin effect (R_{skin}) is calculated [14]as

$$R_{\text{skin}} = \left(\frac{1}{4} + \frac{w}{4\delta} + \frac{6}{32}\frac{\delta}{w}\right) R_{\text{dc}} \tag{1}$$

where δ is the skin depth and R_{dc} is the DC resistance of the coils

$$\delta = \sqrt{\frac{1}{\pi f_0 \mu_0 \sigma}} \quad R_{\text{dc}} = \frac{l}{\pi (w/2)^2 \sigma} \tag{2}$$

and where σ is the conductivity of the wire, f_0 is an operating frequency, μ_0 is the permeability in vacuum, and l is the total length of the spiral coil

$$l = 2\pi \sum_{i=1}^{N_1} \left[\frac{d_{o1}}{2} - (i-1) p_1\right] + 2\pi \sum_{j=1}^{N_2} \left[\frac{d_{o1}}{2} - (N_1 - 1) p_1 - j p_2\right] \tag{3}$$

Next, the ratio of R_{prox} to R_{skin}, called a proximity factor (G_p), is used to calculate the resistance (R_{prox}) due to the proximity effect [13]

$$G_P = \frac{R_{\text{prox}}}{R_{\text{skin}}} = \frac{8\pi^2 \delta^2 x^3 (x-1)}{(2x+1)^2 + 2} \left(\frac{1}{N} \sum_{m=1}^{N} \frac{H_m^2}{I_o^2}\right) \tag{4}$$

where $N = N_1 + N_2$, $x = w/\delta$, I_o is the current of each wire, and H_m is the equivalent total H-field applied to the m^{th} wire from the other wires, which is a function of the number of turns N_1 and N_2, and pitches between turns p_1 and p_2. The detailed expression of H_m can be found in Ref. [14].

Finally, the total AC resistance (R_{coil}) can be expressed as

$$R_{\text{coil}} = R_{\text{skin}} + R_{\text{prox}} = R_{\text{skin}} (1 + G_P) \tag{5}$$

2.2 Inductance

The equivalent inductance of the proposed coil (L_{coil}) can be calculated by considering two inductances connected in series. Thereby, L_{coil} is described as follows

$$L_{\text{coil}} = L_1 + L_2 + 2\sum_{i=1}^{N_1} \sum_{j=1}^{N_2} M_{ij} \tag{6}$$

where L_1 and L_2 are self-inductances of the outside wires and inside wires, respectively, M_{ij} is the mutual inductance between the ith wire and jth wire, as depicted in Fig. 1.

To calculate the equivalent inductance L_{coil}, L_1 and L_2 can be calculated first by using the method of Ref. [15].

$$L_n = \frac{\mu_0 N_n^2 (d_{on} + d_{in})}{4}\left[\ln\left(\frac{2.46}{\varphi_n}\right) + \varphi_n^2\right] \tag{7}$$

where n = 1 or 2, d_{on} and d_{in} are the outer and inner diameters of the coil, respectively, as shown in Fig. 1, and

$$\varphi_n = \frac{d_{on} - d_{in} + 2w}{d_{on} + d_{in}} \tag{8}$$

Second, the mutual inductance between i^{th} and j^{th} turns was calculated by Ref. [16] as

$$M_{ij} = \mu_0 \sqrt{r_i r_j}\,\frac{2}{\alpha}\left[(1 - \frac{\alpha^2}{2})K(\alpha) - E(\alpha)\right] \tag{9}$$

where

$$\alpha = \sqrt{\frac{4 r_i r_j}{(r_i + r_j)^2}} \tag{10}$$

and where $K(\alpha)$ and $E(\alpha)$ are the complete elliptic integrals of the first and second kind, respectively [17], r_i and r_j are the radii of ith and jth turns, respectively.

The total mutual inductance between the outside wires and inside wires M_{12} can be simplified by

$$M_{12} = \sum_{i=1}^{N_1}\sum_{j=1}^{N_2} M_{ij} \approx$$

$$N_1 N_2 \mu_0 \sqrt{r_{a1} r_{a2}}\,\frac{2}{\alpha}\left[\left(1 - \frac{\alpha^2}{2}\right)K(\alpha) - E(\alpha)\right] \tag{11}$$

Where, r_{a1} and r_{a2} are the average radii of the outside wires and inside wires, respectively.

2.3 Correction of equations

The effects of the reverse current and coil curvature on the proximity factor G_p are not considered [5], and the influences of the nonuniform current distribution caused by the skin and proximity effects are ignored in Ref. [15]. Therefore, calculation of the resistance and inductance of compact coils formulas (5) and (6) require modification.

Based on the comparison of the calculation with the FEM simulation results, the correct factors C_R and C_{Ln} (n = 1, 2) for formulas (5) and (6) were found by using a curve-fit method.

$$C_R = 1.013 + 0.351 \times 0.977^{\left(\frac{d_{i2}}{w}\right)} \tag{12}$$

$$C_{Ln} = 0.388\,65\left(\frac{w}{p_n}\right)^{-0.116\,71} + 0.532\,57 \tag{13}$$

Therefore, the modified expressions for the resistance and inductance of the coil can be derived as

$$R_C = C_R R_{skin}(1 + G_P) \tag{14}$$

$$L_C = C_{L1} L_1 + C_{L2} L_2 + 2\sum_{i=1}^{N_1}\sum_{j=1}^{N_2} M_{ij} \tag{15}$$

To validate the modified expressions, the resistances and inductances calculated by formulas (14) and (15) are compared with simulated results and with the results obtained by formulas (5) and (6), respectively, as shown in Fig. 2. For the simulation, a commercial electromagnetic FEM simulator (ANSYS Maxwell 2-D) was used and the geometry mode of the cylindrical about the z-axis was chosen.

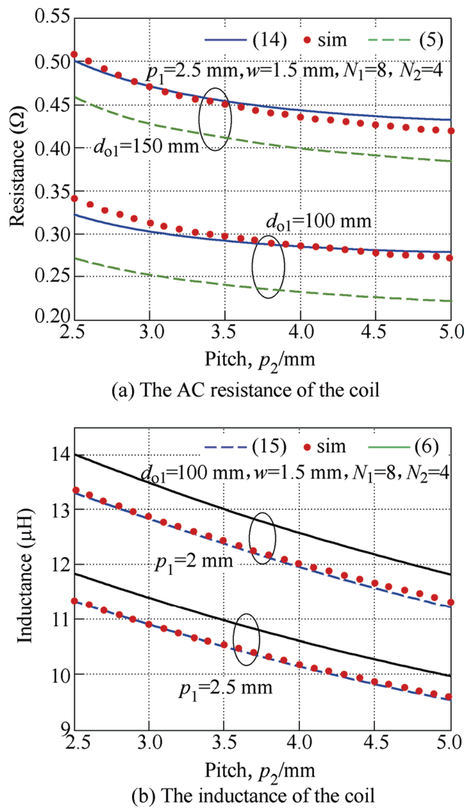

Fig. 2 Comparison of the modified calculation, simulation, and the results obtained by formulas (5) and (6) of the AC resistance and inductance according to the pitches p_2

Fig. 2a shows that the AC resistances calculated by formula (14) agree with the simulation results. However, the results obtained by formula (5) are lower, and the difference increases as the diameter of the coil d_o decreases, which is caused by the effect of the reverse current for a compact coil. It can be observed that the calculated inductances using formula (15) are also consistent with the simulation results, as shown in Fig. 2b. Compared with the results obtained by formula (6), our results are smaller. In addition, the difference becomes greater with a lower p_1/w. Therefore, the nonuniform current distribution caused by the skin and proximity effects should be considered in calculating the inductance for a compact coil.

2.4 Quality factor

According to formulas (14) and (15), the Q-factor of the proposed coil can be obtained as follows

$$Q = \frac{2\pi f_0 L_C}{R_C} \tag{16}$$

Now, we can use this expression to optimize coil design to achieve a high Q-factor.

3 Optimization of the planar spiral coils

As illustrated in Fig. 1, the pitches of the inner turns p_2 are designed to be larger than those of the outer turns p_1, to enhance the magnetic field at the central region of coils, for generating a much more uniform magnetic field than traditional equally-spaced coils [7,18]. According to formula (6), in the case of the same number of turns of the coil, the inner-sparse structure reduces the inductance of the coil compared with a conventional coil, as shown in Fig. 2b. Fortunately, this structure also reduces the influence of the proximity effect, especially for compact coils operating above MHz frequencies, which can reduce the AC resistance of the coil, as depicted in Fig. 2a.

Therefore, the problem turns to one of how the number of turns N_1 and N_2, and pitches between turns p_1 and p_2, are optimized. As a result, the decrease of the resistance can offset the reduction of the inductance. By this method, the proposed coil can maintain a high Q-factor as well as a uniform magnetic field distribution. In this study, we set the outer diameter d_{o1}, wire diameter of coils w, and operating frequency f_0 as, d_{o1} = 100 mm, w = 1.5 mm, and f_0 =1 MHz, which can vary based on the application situation. Therefore, the optimized problem can be summarized as

$$\begin{aligned} &\max \quad Q(N_1, N_2, p_1, p_2) \\ &\text{s.t.} \quad \begin{cases} 2(N_1-1)p_1 + 2N_2 p_2 + w < d_{o1} \\ p_2 > p_1 > w \end{cases} \end{aligned} \tag{17}$$

3.1 Optimal design of TX-coil for a high quality factor

Fig. 3 displays the calculated Q-factor of the proposed coil according to N_1 and N_2 when p_1 = 2 mm and p_2 = 4 mm. It can be seen that the Q-factors of the coil increases first as the number of turns increases; however, when the number of turns increases above a certain value, the Q-factors do not increase any further due to the serious increase of the resistance R_{coil}. It can be clearly shown that the optimal number of outer turns and inner turns for the maximum Q-factor are N_1 = 8 and N_2 = 4, respectively.

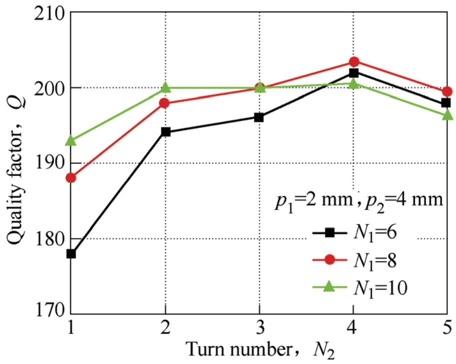

Fig. 3 Calculated Q-factor of the proposed coil according to N_1 and N_2

Fig.4 shows the calculated and simulated Q-factors with different pitches p_1 and p_2, when N_1 = 8 and N_2= 4. It can be observed that the calculation provides a good agreement with the simulation, and there are optimal pitches to maximize the Q-factor. Thus, the optimum pitches p_1 and p_2 are found to be 2.5 mm and 4 mm, respectively, to obtain the maximum Q-factor.

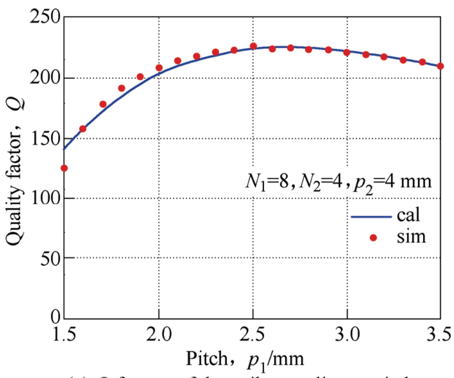

(a) Q-factors of the coil according to pitch p_1

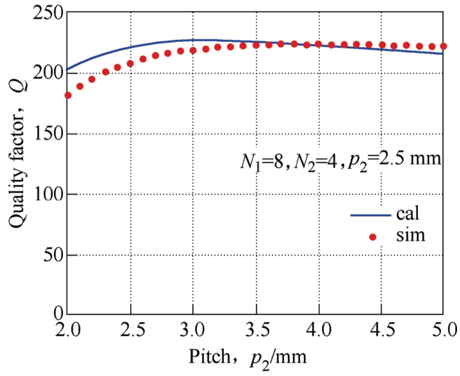

(b) Q-factors of the coil according to pitch p_2

Fig. 4 Calculated and simulated quality factors with different pitches p_1 and p_2

3.2 Optimal design of TX-coil for a uniform magnetic field distribution

Next, we analyzed the magnetic field distribution to finally determine the parameters. Fig. 5 shows the magnetic field intensity with different pitches p_1 and p_2 at 8 mm from the coil when I_o is set to 1 A. Compared with an evenly spaced planar spiral coil, the magnetic field of the proposed coil with an outer-tight and inner-sparse configuration has much better uniformity. Fortunately, the optimized coil with N_1 = 8, N_2 = 4, p_1 = 2.5 mm, and p_2 = 4 mm has not only a high Q-factor but also a uniform magnetic field, as shown in Fig. 5. It is noted that there is a tradeoff between maximum Q-factor and the uniform Magnetic field. Thus, the optimal values can be derived as N_1=8, N_2 = 4, p_1 = 2.5 mm, and p_2 = 4 mm.

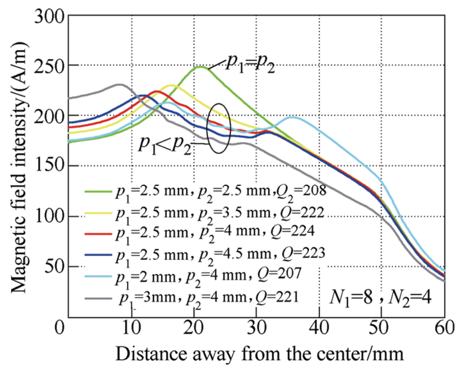

Fig. 5 Magnetic field intensity with different pitches p_1 and p_2 when N_1 = 8 and N_2 = 4

4 Simulation and experimental results

As shown in Fig. 6, five fabricated coils made of solid copper wires are considered for comparison. In these coils, the outer diameter d_{o1} is fixed at 100 mm, the wire diameter of the coils is set to 1.5 mm, and the number of outer turns and inner turns are set as N_1 = 8 and N_2 = 4, respectively. The other parameters of the coils are summarized in detail in Tab. 1, and the resistances, the inductances, and the Q-factors of the coils are measured with a precision impedance analyzer (WAYNE KERR 6500B) at 1 MHz. It can be found that the measured results of the resistances and inductances are basically consistent with the calculated and simulated results. The slight differences between measurement and calculation are due to manufacturing error and a nonideal test environment, for example the parasitic capacitance between the coil and the impedance analyzer. In addition, the model of the concentric multiloop coil used in the calculation makes the inner diameters d_i of the coil slightly larger than those of the spiral coil. However, as the pitches change, the general trend of measurement is consistent with the calculated and simulated results. It can be observed that the measured Q-factors at p_1 = 2.5 mm and p_2 = 4 mm are also maxima. The Q-factor is 200 for #2, which is increased by about 8% in comparison with that of evenly spaced planar spiral coils.

On the basis of the optimized results, the finite element simulation model of the coils was built using Ansys Maxwell 2-D, and the geometry mode of the cylindrical about the z-axis was chosen. Fig.7 illustrates the magnetic field distribution of a conventional evenly-spaced coil and the optimized proposed coil. The proposed optimized coil exhibits a more uniform magnetic field distribution.

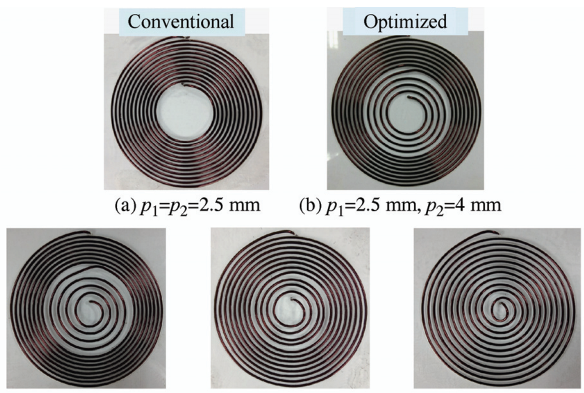

(a) p_1=p_2=2.5 mm (b) p_1=2.5 mm, p_2=4 mm

(c) p_1=2.5 mm, p_2=5 mm (d) p_1=3 mm, p_2=4 mm (e) p_1=3.5 mm, p_2=4 mm

Fig. 6 Fabricated spiral TX-coils with different pitches p_1 and p_2

Tab.1 Parameters of fabricated coils

Coil type	Pitch /mm	Resistance /Ω			Inductance /μH			*Q*-factor		
		Cal	Sim	Mea	Cal	Sim	Mea	Cal	Sim	Mea
#1	p_1=2.5 p_2=2.5	0.322	0.342	0.358	11.34	11.34	10.65	221	208	186
#2	p_1=2.5 p_2=4	0.285	0.286	0.300	10.18	10.15	9.55	223	224	200
#3	p_1=2.5 p_2=5	0.278	0.272	0.286	9.60	9.53	8.94	215	222	196
#4	p_1=3 p_2=4	0.243	0.244	0.268	8.58	8.57	8.15	222	221	191
#5	p_1=3.5 p_2=4	0.216	0.214	0.227	7.24	7.18	6.48	210	210	179

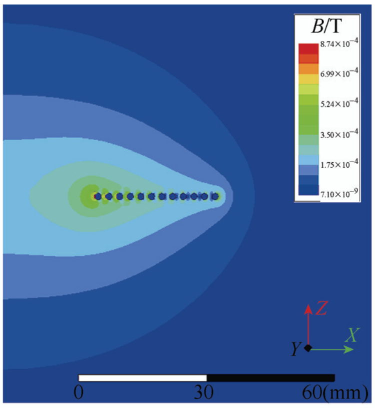

(a) Evenly-spaced coil with N=12, p=2.5 mm, and Q=208

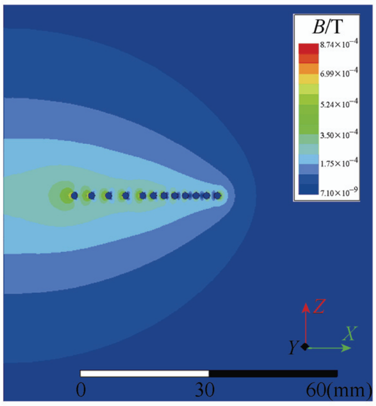

(b) Optimized coil with N_1=8, N_2=4, p_1=2.5 mm, p_2=4 mm, and Q=224

Fig. 7 Magnetic field distribution of the conventional evenly spaced coil and the optimized coil

5 Conclusions

In this study, a novel TX-coil with an outer-tight and inner-sparse configuration was proposed to provide an optimal *Q*-factor and uniform magnetic field. In addition, a closed-form expression of the *Q*-factor including the skin effect and proximity effect was derived for the coil optimization. The proposed optimization process had a much lower computational cost compared to FEM, and can be extended to a wide range of practical WPT applications under certain coil geometry constraints.

References

[1] D Patil, M K McDonough, J M Miller, et al. Wireless power transfer for vehicular applications: overview and challenges. *IEEE Transactions on Transportation Electrification*, 2018, 4(1): 3-37.

[2] A Ahmad, M S Alam, R. Chabaan. A comprehensive review of wireless charging technologies for electric vehicles. *IEEE Transactions on Transportation Electrification,* 2018, 4(1): 38-63.

[3] L Li, H Liu, H Zhang, et al. Efficient wireless power transfer system integrating with metasurface for biological applications. *IEEE Transactions on Industrial Electronics*, 2018, 65: 3230-3239.

[4] J Moon, H Hwang, B Jo, et al. Design and implementation of a high-efficiency 6.78 MHz resonant wireless power transfer system with a 5W fully integrated power receiver. *IET Power Electronics*, 2017, 10(5): 577-587.

[5] D H Kim, J Kim, Y J Park. Optimization and design of small circular coils in a magnetically coupled wireless power transfer system in the megahertz frequency. *IEEE Transactions on Microwave Theory and Techniques*, 2016, 64(8): 1-12.

[6] A L F Stein, P A Kyaw, C R Sullivan. Wireless power transfer utilizing a high-q self-resonant structure. *IEEE Transactions on Power Electronics*, 2019, 34(7): 6722-6735.

[7] T Kim, G Yun, W Y Lee, et al. Asymmetric coil structures for highly efficient wireless power transfer systems. *IEEE Transactions on Microwave Theory and Techniques*, 2018, 66(7): 3443-3451.

[8] A K RamRakhyani, S Mirabbasi, M Chiao. Design and optimization of resonance-based efficient wireless power

delivery systems for biomedical implants. *IEEE Trans. Biomed. Circuits Syst.*, 2011, 5(1): 48-63.

[9] B H Waters, B J Mahoney, G Lee, et al. Optimal coil size ratios for wireless power transfer applications. Proc. *IEEE Int. Symp. Circuits Syst.*, 2014: 2045-2048.

[10] J Uei-Ming, M Ghovanloo. Design and optimization of printed spiral coils for efficient transcutaneous inductive power transmission. *IEEE Trans Biomed Circuits Syst.*, 2007, 1(3): 193-202.

[11] J J Casanova, Z N Low, J S Lin, et al. Transmitting coil achieving uniform magnetic field distribution for planar wireless power transfer system. Proc. *IEEE Radio Wireless Symp.*, 2009: 530-533.

[12] D Yinliang, S Yuanmao, G Yougang. Design of coil structure achieving uniform magnetic field distribution for wireless charging platform. *4th Int. Power Electron. Syst. App. Conf.*, 2011: 1-5.

[13] W-S Lee, H Lim Lee, K-S Oh, et al. Uniform magnetic field distribution of a spatially structured resonant coil for wireless power transfer. *Applied Physics Letters*, 2012, 100(21): 214105.

[14] K Jinwook, P Young-Jin. Approximate closed-form formula for calculating ohmic resistance in coils of parallel round wires with unequal pitches. *IEEE Transactions on Industrial Electronics*, 2015, 62(6): 3482-3489.

[15] S S Mohan, M D Hershenson, S P Boyd, et al. Simple accurate expressions for planar spiral inductances. *IEEE J. Solid-State Circuits*, 1999, 34(10): 1419-1424.

[16] W S Lee,W I Son, K S Oh, et al. Contactless energy transfer systems using antiparallel resonant loops. *IEEE Trans. Ind. Electron.*, 2013, 60(1): 350-359.

[17] C R Paul. Inductance—loop and partial. Hoboken. NJ: Wiley, 2010.

[18] M Q Nguyen, Z Hughes, P Woods, et al. Field distribution models of spiral coil for misalignment analysis in wireless power transfer systems. *IEEE Trans. Microw. Theory Techn.*, 2014, 62(4): 920-930.

Lihao Wu was born in Gutian, Fujian, China, in 1994. He received a B.S. degree in electrical engineering from Fuzhou University, Fuzhou, China, in 2017. He is currently working toward the Ph.D. degree in power electronics at the School of Electric Power, South China University of Technology, Guangzhou, China.

His research interests include wireless power transfer applications and power electronic converters.

Bo Zhang (M'03-SM'15) was born in Shanghai, China, in 1962. He received a B.S. degree in electrical engineering from Zhejiang University, Hangzhou, China, in 1982, an M.S. degree in power electronics from Southwest Jiao Tong University, Chengdu, China, in 1988, and a Ph.D. degree in power electronics from the Nanjing University of Aeronautics and Astronautics, Nanjing, China, in 1994.

He is currently a professor with the School of Electric Power, South China University of Technology, Guangzhou, China. He has authored or co-authored six books published by IEEE-Wiley and Springer, over 450 technical papers, and he holds 100 patents. His current research interests include nonlinear analysis, modeling, and control of power electronic converters and wireless power transfer applications.